

Tricks of the Trade: Selected Li-ion Battery Modeling Techniques

A Thesis

Presented to

The Faculty of the Department of Mechanical Engineering

University of Houston

In Partial Fulfillment

Of the Requirements for the Degree

Bachelor

In Mechanical Engineering

By

Dwight Theriot

December 2018

## Tricks of the Trade: Selected Li-ion Battery Modeling Techniques

---

Dwight Theriot

Approved:

---

Chair of the Committee  
Haleh Ardebili, Associate Professor  
Mechanical Engineering

Committee Members:

---

Ralph Metcalfe, Professor  
Mechanical Engineering

---

Leonard Trombetta, Associate  
Department Chair  
Electrical & Computer Engineering

---

Suresh Khator, Associate Dean  
Cullen College of Engineering

---

Pradeep Sharma, Department Chair  
Mechanical Engineering

Tricks of the Trade: Selected Li-ion Battery Modeling Techniques

An Abstract

of a

Thesis

Presented to

The Faculty of the Department of Mechanical Engineering

University of Houston

In Partial Fulfillment

Of the Requirements for the Degree

Bachelor

In Mechanical Engineering

By

Dwight Theriot

December 2018

## Abstract

Li-ion cells are used in countless applications today, and their use will only increase in the future. It is crucial for researchers to be able to model Li-ion behavior in order to protect consumers, manufacturers, and equipment from the potentially catastrophic effects of thermal runaway, while delivering a high-performance energy storage solution. This paper presents the most widely used methods for modeling Li-ion cells in an easy-to-read fashion, in order to provide a “one-stop-shop” for researchers developing and refining new models. Models are categorized into empirical and analytical models, and seminal studies for each are laid out in detail, as well as modifications that enhance their utility and/or efficiency. Thermal runaway models are presented in detail, including various triggering mechanisms. Summary tables presented here will allow researchers to quickly review existing literature in order to identify knowledge gaps and models which can be used for a variety of applications.

# Table of Contents

<b>ABSTRACT</b> .....	<b>V</b>
<b>TABLE OF CONTENTS</b> .....	<b>VI</b>
<b>LIST OF FIGURES</b> .....	<b>VII</b>
<b>LIST OF TABLES</b> .....	<b>VIII</b>
<b>CHAPTER 1. INTRODUCTION</b> .....	<b>1</b>
1.1 BACKGROUND AND MOTIVATIONS .....	1
1.2 RESEARCH OBJECTIVES AND METHODOLOGY .....	3
1.3 OVERVIEW OF THIS THESIS.....	4
<b>CHAPTER 2. MODELING LI-ION CELLS</b> .....	<b>5</b>
2.1 EMPIRICAL THERMAL MODELING .....	7
2.2 ELECTROCHEMICAL MODELING.....	11
2.2.1 Multi-scale, Multi-dimensional (MSMD) Model .....	13
2.2.2. Reduced Order Model (ROM).....	14
2.3 THERMAL RUNAWAY MODELING .....	15
2.3.1 Empirical-based Thermal Runaway Models .....	15
2.3.2 Analytical-based Thermal Runaway Models .....	16
2.3.3. Thermal Runaway Number .....	17
<b>CHAPTER 3. SUMMARY TABLES</b> .....	<b>18</b>
<b>CHAPTER 4. APPLICATION</b> .....	<b>42</b>
<b>CHAPTER 5. CONCLUSIONS AND FUTURE WORK</b> .....	<b>44</b>
5.1 CONCLUSIONS .....	44
5.2 FUTURE WORK.....	44
<b>REFERENCES</b> .....	<b>45</b>

## List of Figures

Figure 1. Ragone plot showing Li-ion battery energy density in comparison with other power delivery and storage systems.....	1
Figure 2. Block diagram for empirical modeling techniques. ....	7
Figure 3. Block diagram for the pseudo-2D model. ....	11

## List of Tables

Table 1. Seminal Studies .....	18
Table 2. Empirical Models.....	19
Table 3. Analytical/P2D Models .....	22
Table 4. Thermal Runaway Models.....	23
Table 5. Battery Management System (BMS) Models .....	28
Table 6. All models (alphabetical order).....	32

# Chapter 1. Introduction

## 1.1 Background and Motivations

Since Sony's release of the first commercial Lithium-ion (Li-ion) in 1991<sup>1</sup>, the global demand for Li-ion batteries has grown dramatically. Today, Li-ion batteries are found in countless devices, ranging in scale from portable electronics such as wireless headphones, cell phones, and portable power tools, to large-scale systems such as electric cars and off-grid energy storage. Lithium is the most electropositive and lightest metal which makes it an ideal candidate for creating lightweight energy-dense batteries. Due to their rapid increase in demand and development Li-ion battery capacity has nearly doubled since their commercial debut (from 110 W h kg<sup>-1</sup> to 200 W h kg<sup>-1</sup>).<sup>1</sup> The suitability of Li-ion batteries as excellent candidates for energy-dense storage applications is readily apparent due to its position on the Ragone plot, shown in Figure 1.

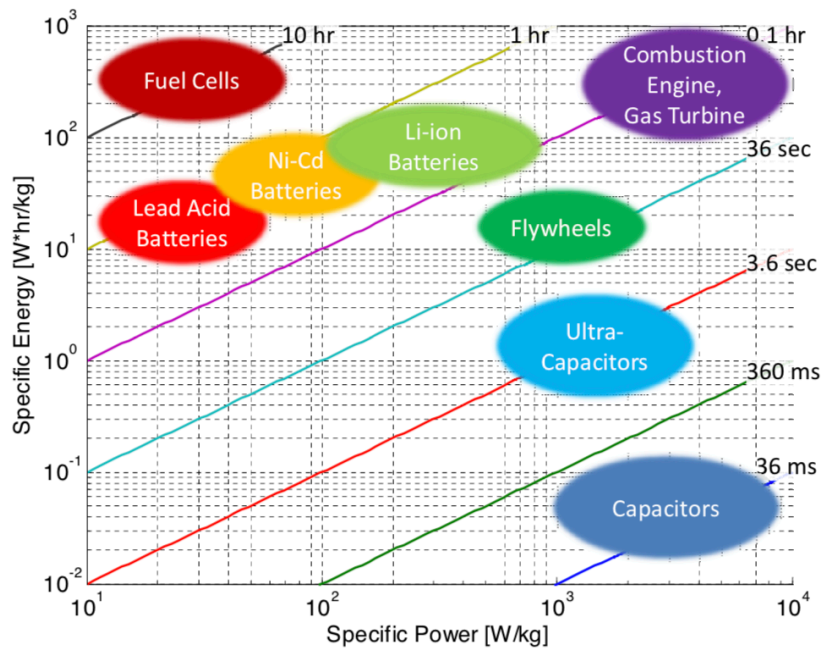


Figure 1. Ragone plot showing Li-ion battery energy density in comparison with other power delivery and storage systems.<sup>2</sup>

Because of their light weight and high capacity, Li-ion batteries can be found in applications where energy density is paramount, such as electric vehicles. Auto manufacturers such as Tesla and General Motors (GM) continue to develop electric cars with improved range and capacity, which is the primary selling point for consumers when considering an all-electric vehicle. Tesla continues to create new models of electric cars each year boasting higher ranges, and GM recently announced that 20 of their models will be fully electric by the year 2023.<sup>3</sup> The market share of all-electric vehicles is steadily increasing, and even if the electricity used to charge those vehicles is derived from fossil-fuel burning power plants, carbon emissions could decrease by 28% in the US over a ten-year period at a gas-to-electric vehicle conversion rate of 10% per year.<sup>4</sup> Additionally, if every passenger car and light-duty truck in the US were instantaneously converted to an electric vehicle, the total emissions reduction would be a staggering 58% in the same time period.<sup>4</sup>

As scientists and engineers continue to innovate new products and solutions which require compact high-density energy storage, the need for ensuring these systems remain safe for consumers has never been more relevant. Developments in Li-ion battery safety have advanced significantly in the past few decades, however, the demand for their use seems to have outpaced our collective ability to model and understand these systems in sufficient detail to completely avoid disastrous results. The most significant safety consideration when using Li-ion batteries is thermal runaway, which is when a battery enters a positive feedback thermal cycle and generates more heat than it can dissipate, and without the proper controls results in an exothermal decomposition of its materials,

thus creating a fire, explosion, and ejection of hot toxic materials.<sup>5</sup> Thermal runaway can be triggered by a myriad of mechanisms including (a) overheating, (b) external or internal short circuit, (c) penetration, (d) crushing, (e) cell-to-cell propagation, and (f) leakage.<sup>6</sup> Leading battery technology corporations have not been able to completely avoid the pitfalls of improper Li-ion battery safety and implementation, leading to numerous high-profile, costly failures and recalls of Li-ion batteries installed in their devices. For example, in 2016 Samsung discontinued and recalled the Note 7 smartphone less than one month after its initial release due to thermal runaway occurring in the phone's battery caused by a manufacturing defect.<sup>7</sup>

Although some investigators believe that Li-ion batteries have or will soon reach their peak performance<sup>8</sup>, and recently developed batteries such as Li-S, K-ion and Na-ion may be able to deliver energy densities up to five times that of Li-ion batteries<sup>9</sup>, further research into thermal modeling of Li-ion batteries will enable researchers to develop the tools necessary to safely produce and implement Li-ion batteries and more energy-dense batteries in the future.

## 1.2 Research Objectives and Methodology

The objective of this research is to present battery modeling techniques, focusing on models which can characterize and predict thermal runaway, and to present those models in an easy-to-read fashion in order to readily identify knowledge gaps and for use as a reference. The methodology used here began by finding Li-ion cell models commonly cited in literature, including heat generation, heat transfer, and electrochemical models, and how those models have been developed by others.

### 1.3 Overview of this thesis

This thesis presents and reviews the mathematical models that have been developed to describe the thermal and electrochemical behavior of Li-ion batteries. First, empirical models are presented, as they are the most common method to quickly and accurately model cell behavior verified by experiment. Then, analytical electrochemical models are presented, as well as multi-dimensional and reduced-order models based on analytical models. Analytical and empirical models that address thermal runaway triggering mechanisms, or combinations of mechanisms, have been highlighted as well.

Certain models were selected by their high frequency of citation in order to highlight current and past trends in the field. Because heavy emphasis is placed on analyzing various combinations of materials for electrodes and electrolytes, those materials will also be listed in detail. Models which do not include thermal runaway will also be included, as these models are necessary for developing thermal runaway models. Fast and efficient models that are or can be used for real-time Battery Management Systems (BMS) are highlighted as well. Models presented in this paper are summarized in table format in Chapter 3.

## Chapter 2. Modeling Li-Ion Cells

The temperature at which Li-ion batteries operate dictates their chemical performance, measured by capacity and power fade over many discharge cycles, overall life, power delivery, safety, thermal runaway potential, self-discharge, low-temperature performance, and electrical balance across cells.<sup>10</sup> It is essential for investigators to be able to model cells using novel electrode materials and electrolyte combinations, not only in order to avoid repetitive and costly calorimetry testing, but to also develop the proper controllers and safety mechanisms for BMS to keep developed batteries operating safely at their peak performance.

Many types of models have been developed, each with their own applications based primarily on their expediency and level of detail they can provide. For instance, some models seek to characterize the molecular transport phenomenon associated with a battery's chemistry, and others seek to address the overall behavior and performance of an entire cell or group of cells (a "cell" refers to a single anode/cathode/electrolyte package, whereas a "battery" can refer to a single cell or group of cells). Generally, models can be categorized by their foundation, application, scale, dimensionality, coupled or non-coupled physics, cell chemistry, and triggering mechanisms, among other parameters.

Lumped and 1D Models for analyzing cells can be relatively simple, expedient, and provide the level of detail necessary to achieve practical results for single cylindrical or prismatic cells, however, experimental data confirmed with multi-dimensional, multi-physics models are essential for allowing investigators to develop large-format batteries.<sup>11</sup> In addition, the thermophysical properties of the cell materials must be known

in order to achieve an accurate model, for instance, the thermal conductivity in the direction of the electrode surface as well as perpendicular to it, and those properties may not be readily available in literature which would require experimental testing to achieve.<sup>11</sup> Additionally, many thermophysical properties are functions of temperature, and there are a myriad of approaches in literature for addressing this temperature dependency. Thermal runaway models differ in that there are many more parameters and often chaotic phenomena to consider, such as Joule-Thompson cooling during thermal runaway venting<sup>12</sup>, and are constantly being developed and compared to experimental data.

Many practical applications can be simulated using lumped models, however, higher fidelity is often necessary to address safety and performance concerns when designing battery systems. The aforementioned models assume that cell components behave isothermally, and therefore are not able to identify “hot spots.” Experiments and thermo-electrochemical analysis have shown that there are asymmetric temperature distributions within cells and systems during nominal thermal testing and abuse testing.<sup>13</sup> By extending the lumped models to multiple dimensions, we begin to understand the effects of cell geometry, placement of cell components, selection of cell chemistry and separators, interstitial heat sink/insulation materials, effects of localized heating and cooling, non-uniform spatial distributions, cell-to-cell propagation, and thermal and electrical conductive paths within a cell. For instance, spirally-wound cells have different thermal conductivities axially and radially (through jelly roll layers), which has a large impact on how heat is conducted and dissipated throughout the cell as the temperature is raised. Extension to multiple dimensions allows for model development of all types of

form factors, which is especially important for larger format cells and batteries due to their smaller surface-to-volume ratio and higher thermal resistance. Due to their complexity, current work is focused on building robust models that can deliver accurate results while minimizing computational burden, utilizing techniques such as symmetry.

## 2.1 Empirical Thermal modeling

Thermal modeling can be generally divided into two categories, which are heat generation and heat transfer, as depicted in Figure 2.

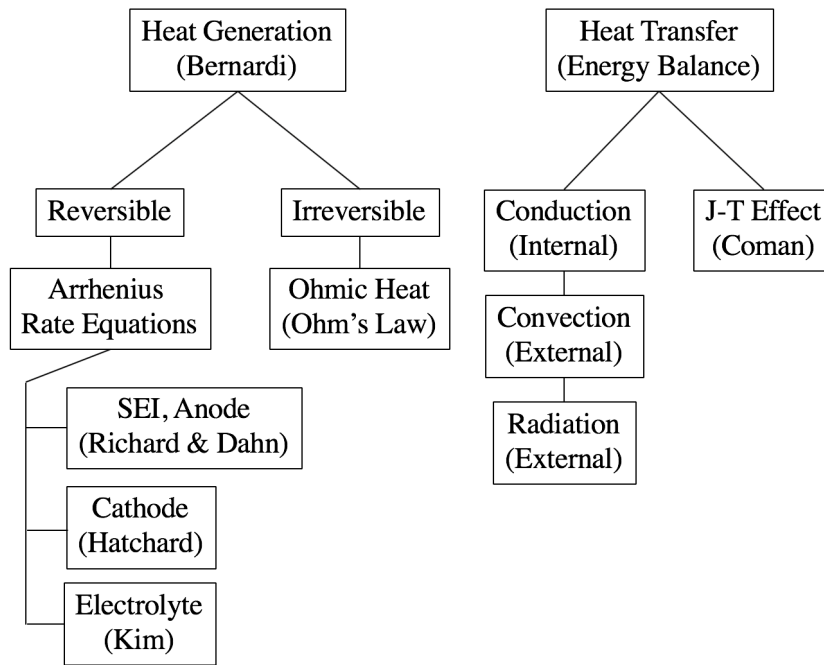


Figure 2. Block diagram for empirical modeling techniques.

Heat generation models consider reversible and irreversible heat generation within a cell according to electrochemical reaction rates and are typically dependent on the cell's open-circuit voltage or State of Charge (SoC). Heat transfer modeling consists of analytical solutions to conduction, radiation, and convection equations with appropriate

boundary conditions. Heat generation and transfer models are typically coupled by the electrochemical heat generation rate, especially for multi-dimensional models, Battery Management Systems (BMS), and studies on the effectiveness of various cooling or insulation systems.

The most commonly cited heat generation model used in Li-ion battery modeling was developed by Bernardi et al., who derived an expression for heat generation within a single complete cell based on an energy balance formulated by combining the first law of thermodynamics with a previously reported model based on Joule heating by Sherfey and Brenner.<sup>14</sup> This expression formulates the internal heat generation as a function of (a) time, (b) electrical work, (c) heat transfer with the cell's surroundings, (d) transients in the heat capacity of the system, (e) chemical reactions, (f) mixing, and (g) phase changes,<sup>15</sup> and is commonly cited in the following simplified form to include only the primary thermal drivers, neglecting phase change and mixing effects:

$$Q_{cell} = I \left( V_{OC} - V_W - T \frac{\partial V_{OC}}{\partial T} \right), \quad (1)$$

where  $Q$  [W] is the heat transfer rate,  $I$  [I] is cell current,  $V_{OC}$  [V] is the open circuit potential,  $V_W$  [V] is the working potential, and  $T$  is the absolute temperature. In Eq. (1), the  $V_{OC}$  and  $V_W$  terms account for Ohmic losses, and the derivative term is the entropic heat coefficient. Bernardi's model only accounts for nominal cell operations, which is why the model cannot be used directly for thermal runaway modeling.

Richard and Dahn conducted accelerating rate calorimetry (ARC) experiments on Li-ion battery anode and SEI materials in order to develop a model which calculates self-heating rates of the decomposition of these materials, and is subsequently able to accurately predict differential scanning calorimetry (DSC) profiles.<sup>16</sup> Richard and Dahn

employed Arrhenius-like expressions which account for the temperature dependence on the rate of SEI and anode decomposition reactions, the change in the amounts of the reactants and products, and the associated heat generation which is a function of the decomposition rates, which are described as follows:

$$\frac{dx_{SEI}}{dt} = -A_{SEI}x_{SEI} \exp\left(\frac{-E_{SEI}}{k_bT}\right), \quad (2)$$

$$\frac{dx_a}{dt} = -A_a x_a \exp\left(\frac{-z}{z_0}\right) \exp\left(\frac{-E_a}{k_bT}\right), \quad (3)$$

$$\frac{dz}{dt} = A_a x_a \exp\left(\frac{-z}{z_0}\right) \exp\left(\frac{-E_a}{k_bT}\right), \quad (4)$$

$$\frac{dQ_{SEI}}{dt} = -m_{SEI}h_{SEI} \frac{dx_{SEI}}{dt}, \text{ and} \quad (5)$$

$$\frac{dQ_a}{dt} = -m_a h_a \frac{dx_a}{dt}, \quad (6)$$

where  $x$  represents the fraction of Li ions in SEI and anode,  $A$  is the frequency factor,  $z$  is the SEI thickness,  $E$  is the activation energy,  $k_b$  is the Boltzmann constant,  $T$  is temperature,  $t$  is time,  $Q$  is the heat generated by the decomposition reaction,  $m$  is mass, and  $h$  is the enthalpy; the subscript  $a$  refers to the anode component and subscript  $SEI$  refers to the SEI component.<sup>16,17</sup> Equations (2) and (3) represent the decomposition rates of the anode and SEI layer; Equation (4) represents the change in  $z$ , SEI thickness. Equations (5) and (6) represent the heat generation rate for each material which is a function of their respective decomposition rates. Of note, the only difference between equations (3) and (4) is the negative sign on the right-hand sides. This difference ensures that  $z$  increases as  $x_a$  decreases, which is indicative of the SEI becoming proportionately thicker as lithium decomposes, which in turn decreases the amount of available lithium for reaction, thus affecting the respective rates of heat generation of each over time. This

model only considered anode and SEI reactions, and the heat generated by the exothermic decomposition of other cell components must be accounted for as well.

Hatchard et al. formulated a model which incorporates cathode decomposition<sup>18</sup>, which is described with two additional equations as:

$$\frac{dx_c}{dt} = A_c x_c (1 - x_c) \exp\left(\frac{-E_c}{k_b T}\right) \text{ and} \quad (7)$$

$$\frac{dQ_c}{dt} = m_c h_c \frac{dx_c}{dt}, \quad (8)$$

where the subscript c represents the fraction of Li ions in the cathode and all other variables follow the same nomenclature as previously described. Hatchard's model is able to predict radial heat production and flow when the cell is exposed to standard benchmark oven testing with various cathode chemistries, without having to conduct costly physical testing as long as the thermal properties of the electrolyte and cell can be known. A numerical lumped parameter model for an 18650 cell presented by Hatchard, which builds on Richard and Dahn's model, is often used as a foundation for developing more complex models by expanding to multiple dimensions.

Kim et al. later described electrolyte decomposition using the following two equations:

$$\frac{dY_e}{dt} = -A_e Y_e \exp\left(\frac{-E_e}{k_b T}\right) \text{ and} \quad (9)$$

$$\frac{dQ_e}{dt} = -m_e h_e \frac{dY_e}{dt}, \quad (10)$$

where Y is the fraction of remaining electrolyte and all other variables follow the same nomenclature as previously described.

Using the aforementioned equations and the transient heat conduction equation, which is written as

$$\rho c_p \frac{\partial T}{\partial t} = \nabla(k_j \nabla T) + Q = \frac{\partial}{\partial x} \left( k_x \frac{\partial T}{\partial x} \right) + \frac{\partial}{\partial y} \left( k_y \frac{\partial T}{\partial y} \right) + \frac{\partial}{\partial z} \left( k_z \frac{\partial T}{\partial z} \right) + Q, \quad (11)$$

where  $k$  is the thermal conductivity, and  $Q$  is the sum of heat generation terms, the thermal behavior at any point in the cell can be predicted.

## 2.2 Electrochemical Modeling

Whereas the Arrhenius equations presented in Section 2.1 represent reaction rates formulated from calorimetry experiments, the following models seek to address the electrochemical behavior of a cell based on an analytic solution.

The most commonly cited electrochemical model is the pseudo-2D model (P2D), developed by Doyle, Fuller, and Newman and published in 1993<sup>19</sup>, depicted by the block diagram in Figure 3.

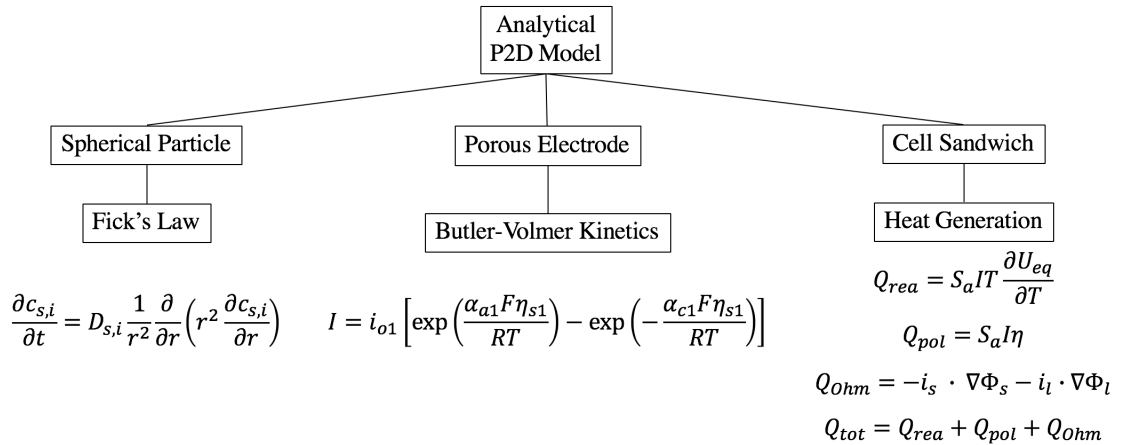


Figure 3. Block diagram for the pseudo-2D model.

The authors utilized concentrated solution theory in order to model transport of various cell constituents in a lithium/polymer/insertion cell, as well as predicted the cell's voltage, concentration profiles, and pore wall flux at various discharge rates. Discretized cell elements in the through-plane direction constitute the first dimension of the model

and are used to model one-dimensional ion transport from the lithium anode through a polymer separator to the cathode, called a cell “sandwich.”<sup>19,20</sup> By assuming the diffusion particles at the surface of the electrodes are spherical, a material balance is described using Fick’s Second Law of Diffusion, given by

$$\frac{\partial c_{s,i}}{\partial t} = D_{s,i} \frac{1}{r^2} \frac{\partial}{\partial r} \left( r^2 \frac{\partial c_{s,i}}{\partial r} \right), \quad (12)$$

where  $c$  is the concentration of lithium in the solid particle phase (where  $i = p, n$  is for the positive and negative electrodes, respectively), and  $D$  is the diffusion coefficient.<sup>19,21</sup> At the center of the particle the flux is equal to zero, and at its surface the flux is equal to the rate of lithium ion consumption/production occurring at the interface between the solid electrode and liquid electrolyte.<sup>21</sup> The radial direction of the diffusion particles constitutes the second dimension in the P2D model. Charge conservation in the electrode and the electrolyte phase are modeled using Ohm’s Law and coupled via the reaction current, which is dependent on the transport of lithium ions.<sup>22</sup> Lithium ion transport in the electrolyte is developed from the general Butler-Volmer kinetic equation, which describes the current density of the cell as a function of ion transport, the surface overpotential, and the lithium ion concentration in the electrolyte phase is given by

$$I = i_{o1} \left[ \exp \left( \frac{\alpha_{a1} F \eta_{s1}}{RT} \right) - \exp \left( - \frac{\alpha_{c1} F \eta_{s1}}{RT} \right) \right], \quad (13)$$

where  $I$  is the superficial current density (pore wall flux),  $\eta$  is the local value of the surface overpotential,  $F$  is Faraday’s constant, and  $\alpha_{a1}$  and  $\alpha_{c1}$  are the anodic and cathodic charge transfer coefficients.<sup>19,21</sup> Heat generation within a cell is then typically modeled using either Bernardi’s formulation as described previously, or as a sum of the reversible (entropic), irreversible (polarization), and Ohmic heats as follows:

$$Q_{tot} = Q_{rea} + Q_{pol} + Q_{ohm} , \quad (14)$$

$$Q_{rea} = S_a I T \frac{\partial U_{eq}}{\partial T} , \quad (15)$$

$$Q_{pol} = S_a I \eta , \text{ and} \quad (16)$$

$$Q_{ohm} = -i_s \cdot \nabla \Phi_s - i_l \cdot \nabla \Phi_l , \quad (17)$$

where  $S$  is the specific surface area,  $U$  is the open circuit potential,  $I$  is from Eqn. 15,  $i_s$  and  $i_l$  are the variation of potential in the solid and liquid phases respectively, and  $\Phi$  is the potential field.<sup>19,22,23</sup>

Much of the work to develop this model by others has focused on extending the model to multiple spatial dimensions, and to replicate the model's success without paying penalties in computational cost. Selected models developed from the P2D model are highlighted in the following sections.

### 2.2.1 Multi-scale, Multi-dimensional (MSMD) Model

The P2D model assumes the potential in the current collectors is uniformly distributed, and is therefore limited in accuracy when applied to large-format cells and batteries. Pals and Newman first extended the P2D model to include multiple cells in a stack, however, only considered cells isothermally. Recognizing that potential and temperature imbalances can lead to certain areas of large-format cells to be cycled more often than others, Kim et al.<sup>24</sup> developed the MSMD model to account for these differences. The MSMD model allows for computational efficiency while resolving the multi-physics model at the particle, electrode, and cell levels.<sup>24</sup> At the particle level, the charge transfer kinetics and solid-phase lithium diffusion are solved. At the electrode level, the charge balance across the electrode pair as well as lithium ion transport in liquid electrolyte are solved. Lumped variables from the electrode level serve as inputs to

the particle level, such as the liquid phase concentration, electrical potential, and the temperature. At the cell domain level, various cell geometries and battery configurations can be used, lending to the model's versatility. This model was further enhanced by Lee et al.<sup>25</sup> by using the MSMD framework to develop the wound potential-pair continuum (WPPC) model as the cell domain for investigating wound cylindrical cells.

#### 2.2.2. Reduced Order Model (ROM)

Extending the P2D model to multiple spatial dimensions increases computation time significantly, which is an undesirable consequence. In order to efficiently harness the accuracy of the P2D model, Guo et al. developed a linear approximation method which can model the behavior of multiple cells under various nominal charge/discharge operations in a fraction of the time required for the fully-distributed model.<sup>26</sup> The reduced order model, however, still lacks sufficient accuracy for use modeling charge/discharge rates exceeding 5C.<sup>23</sup> The reduced order model decouples the energy balance equation from the P2D model, by focusing on the segregation of computational domains. Whereas in the fully-distributed model a very large system of non-linear differential equations must be solved for each point in the domain, the reduced order model replaces the distributed input variables with volume averages of those variables approximated with a first-order Taylor expansion.<sup>23</sup> Farag et al. developed a ROM by assuming that the lithium concentration in electrolyte is uniform and constant (and therefore the distribution of solid particles is averaged along an electrode surface), and aging parameters were neglected.<sup>27</sup>

## 2.3 Thermal Runaway Modeling

### 2.3.1 Empirical-based Thermal Runaway Models

In order to develop a thermal runaway model, Coman et al. recognized that the Bernardi, Hatchard, and Kim models did not represent key parameters associated with behavior of thermal runaway gases<sup>12</sup>. These missing parameters resulted in differences between simulated events and test data. Coman et al. then constructed a model that builds from the aforementioned models that was designed to account for the boiling, venting, and vaporization of the electrolyte, which dissipates a large amount of the heat produced during thermal runaway due to the Joule-Thomson effect as a function of the SoC of the cell, which is described with the following equation where subscript  $ec$  refers to electrochemical energy and SoC refers to the state of charge of the Li-ion cell:

$$\frac{dSoC}{dt} = -A_{ec}(1 - x_c)x_a \exp\left(\frac{-E_{ec}}{k_b T}\right) + \left(\frac{dx_c}{dt} - \frac{dx_a}{dt}\right)SoC. \quad (18)$$

Venting typically occurs when a cell reaches a critical temperature and/or pressure, and manufacturers have built vents into their cells in order better control the cell's behavior during TR or to prevent TR entirely. Coman's model assumes the vented electrolyte behaves as an ideal gas flowing isentropically through an orifice which opens when the internal cell pressure reaches a critical value. Coman et al. also acknowledged that when TR occurs, all remaining stored electrochemical energy is released into the system in the form of heat (in addition to the heat generated through exothermic decomposition reactions). Therefore an additional equation was introduced as

$$\frac{dQ_{ec}}{dt} = -(m_c + m_a)h_{ec} \frac{dSoC}{dt}. \quad (19)$$

Empirical models have been successful at modeling thermal runaway due to overheating, overpressure, nail penetration (internal short-circuit), and cell-to-cell

propagation. Kim et al. reproduced Hatchard's model and extended it to multiple spatial dimensions and was able to simulate local hot spot development and propagation within a cell, however, internal short circuit was neglected.<sup>28</sup> Recognizing the need to model the internal short circuit due to its large contribution to Ohmic heating due to the very high induced current, Liang et al. developed a method for calculating the short-circuit area equivalent resistance around the nail penetration site to include in the model.<sup>29</sup> Feng et al. developed a thermal runaway model including the internal short-circuit due to nail penetration<sup>6</sup>, as well as cell-to-cell propagation in a large format battery pack.<sup>30</sup>

### 2.3.2 Analytical-based Thermal Runaway Models

Coupled analytic models have been successful at predicting and analyzing thermal runaway, and are better suited to perform certain calculations that empirical models have difficulty modeling. Because empirical models address the reaction rates within a cell based on experiment, the difficulties of modeling phenomenon such as entropic heating due to nail penetration becomes readily apparent due to the difficulties of taking accurate measurements, for instance, the temperature within a cell (without damaging the integrity of the cell to some degree), the equivalent resistance surrounding a nail penetration site, or any other type of mechanical deformation of a cell which may create an internal short circuit. Chiu et al. developed the P2D model to include internal short-circuit, as well as the entropic heating created by the nail reacting with the cell's constituent chemicals.<sup>31</sup> Zhao et al. later included Ohmic heating due to nail penetration.<sup>32</sup> Of note, only analytic models have had success with coupled thermal runaway models induced by mechanical

deformation of the cell. Zhang et al. considered the internal short-circuit as the thermal runaway triggering mechanism while crushing a prismatic pouch cell.<sup>33</sup> Liu et al. developed a mechanical deformation thermal runaway model for cylindrical cells.<sup>34</sup>

### 2.3.3. Thermal Runaway Number

Non-dimensional numbers are useful tools that can assess the holistic behavior of a system using a single factor distilled from various data points. Shah et al.<sup>35</sup> combined conduction, convection, and reaction kinetic considerations into a single factor, the Thermal Runaway Number (TRN), to predict if and when thermal runaway occurs, described as

$$TRN \equiv \frac{\beta R^2}{k_r \mu_1^2} < 1 . \quad (20)$$

The TRN is able to accurately predict when a cell enters thermal runaway in a thermal design space, comparing the convective heat transfer coefficient to the cell's thermal conductivity. The TRN must be less than unity in order to prevent thermal runaway.

## Chapter 3. Summary Tables

This chapter organizes the results of the modeling and literature review and is summarized in table format. Table 1 presents seminal studies that are referenced throughout the remaining tables, and represents the foundation of modeling techniques.

*Table 1. Seminal Studies*

Author	Year	Journal	Title	Type
Bernardi et al. <sup>15</sup>	1985	J. Electrochemical Soc.	A general energy balance for battery systems	Analytical
Chen, et al. <sup>36</sup>	1996	J. Electrochemical Soc.	Thermal analysis of lithium-ion batteries	Analytical
Coman et al. <sup>12</sup>	2016	J. Power Sources	A lumped model of venting during thermal runaway in a cylindrical Lithium Cobalt Oxide lithium-ion cell	Empirical
Doyle et al. <sup>19</sup>	1993	J. Electrochemical Soc.	Modeling of galvanostatic charge and discharge of the lithium/polymer/insertion Cell	Analytical
Gu, W.B.; Wang, C.Y. <sup>37</sup>	2000	J. Electrochemical Soc.	Thermal-electrochemical modeling of battery systems	Analytical
Hatchard, et al. <sup>18</sup>	2001	J. Electrochemical Soc.	Thermal model of cylindrical and prismatic lithium-ion cells	Empirical
Kim, G.H., et al. <sup>28</sup>	2007	J. Power Sources	A three-dimensional thermal abuse model for lithium-ion cells	Empirical
Kim, G.H., et al. <sup>24</sup>	2011	J. Electrochemical Soc.	Multi-domain modeling of lithium-ion batteries encompassing multi-physics in varied length scales	Analytical
Newman, J; Tiedemann, W. <sup>38</sup>	1995	J. Electrochemical Soc.	Temperature rise in a battery module with constant heat generation	Analytical
Pals, C.; Newman, J. <sup>39</sup>	1995	J. Electrochemical Soc.	Thermal modeling of the lithium/polymer battery	Analytical
Rao, L; Newman, J. <sup>40</sup>	1997	J. Electrochemical Soc.	Heat-generation rate and general energy balance for insertion battery systems	Analytical
Richard, M.N.; Dahn, J.R. <sup>16</sup>	1999	J. Electrochemical Soc.	Accelerating rate calorimetry study on the thermal stability of lithium intercalated graphite in electrolyte II	Empirical
Sherfey, J.M.; Brenner, A. <sup>14</sup>	1958	J. Electrochemical Soc.	Electrochemical calorimetry	Empirical
Spotnitz, R. et al. <sup>41</sup>	2003	J. Power Sources	Abuse behavior of high-power, lithium-ion cells	Empirical
Thomas, K; Newman, J. <sup>42</sup>	2003	J. Electrochemical Soc.	Thermal modeling of porous insertion electrodes	Empirical

Tables 2 and 3 are organized from left to right as follows: (a) author, (b) pseudo and/or spatial dimension of the model, (c) reversible heat generation model, (d) irreversible heat generation model, (e) external heat transfer boundary conditions, (f) electrochemical model, (g) multi-physics employed where T=thermal, T/E=thermal+electrical, T-EC=thermo-electrochemical, (h) novelty, (i) cells and/or batteries used in experiment or model, (j) cell/battery geometry where P=prismatic and C=cylindrical, (k) charge/discharge rates, (l) negative electrode composition, (m) electrolyte composition, (n) positive electrode composition.

*Table 2. Empirical Models*

Author	Dim.	Rev. HG	Irr. HG	Ext. B.C.	E.C.	Multi	Novelty	Cells, Batteries	Geo.	C-Rate	-	E.L.	+
Chacko; Chung <sup>43</sup>	3	Bernardi <sup>15</sup>	Bernardi	Convection	Kwon <sup>44</sup> PDE	T-EC	Modified Newman <sup>38</sup> to estimate current density, Seebeck effect, during both charge and discharge	20 Ah single cell	P	0.5, 1.2, 3, 5	C		Li[NiMnCo]O <sub>2</sub>
Chen, S.C., et al <sup>45</sup>	2	Bernardi	Bernardi	Convection (natural, forced parallel & cross flow), Radiation		T/E	Spiral geometry model developed (instead of concentric rings like Hatchard <sup>18</sup> ), radial temperature profile	0.08, 2.16, 10, 27.44, 58.32, 106.48 Ah	C	1, 3	C	Liq	LiCoO <sub>2</sub>

Table 2. Empirical Models (continued)

Author	Dim.	Rev. HG	Irr. HG	Ext. B.C.	E.C.	Multi	Novelty	Cells, Batteries	Geo.	C-Rate	-	E.L.	+
Chen, S.C., et al <sup>36</sup>	1/2/3	Bernardi	Bernardi	Convection (natural, forced), Radiation		T/E	Simplified thermal model with fast computation speed	185.3 Ah Li-ion battery	P	0.2, 1, 2, 3	C	Liq	LiCoO <sub>2</sub>
Damay, et al <sup>46</sup>	0	Reaction	Ohmic	Insulation, Convection		T/E	Uses equivalent circuit for use in BMS microcontroller	40 Ah battery	P	0.5, 2	C		LiFePO <sub>4</sub>
Forgez, et al <sup>47</sup>	0	Thomas <sup>42</sup>	Thomas	HT w/ surround.		T	Simplified thermal model, estimate internal isothermal temperature for use in BMS	26650 single cell	C	6	C		LiFePO <sub>4</sub>
Gumussu, et al <sup>48</sup>	3	Bernardi	Bernardi	Convection		T/E	3D CFD natural convection analysis (external)	Panasonic NCR1865 0B	C	0.5, 1.0, 1.5			
Jeon; Baek <sup>49</sup>	3	Bernardi	Bernardi	Convection	Energy Balance	T/E	Analyzes contributions to entropy change from rev. and irr. sources at various C-rates	1.5 Ah Sony 18650 LiCoO <sub>2</sub> /C	C	0.5, 1, 2, 3, 4, 5	C		LiCoO <sub>2</sub>
Kim, U; Yi, J, et al <sup>50</sup>	2	Bernardi	Bernardi	Convection	Kwon PDE	T-EC	Effect of charge conditions on thermal behavior	14.6 Ah LG Chem.	P	1, 3, 5	C		LiMn <sub>2</sub> O <sub>4</sub>
Nieto, N, et al <sup>51</sup>	0	Bernardi	Bernardi	Convection Radiation		T	Faster discharge rates considered, internal resistance is used to measure overpotential	Tenergy 30123 10.5 Ah cell	P	1, 3, 5			

Table 2. Empirical Models (continued)

Author	Dim.	Rev. HG	Irr. HG	Ext. B.C.	E.C.	Multi	Novelty	Cells, Batteries	Geo.	C-Rate	-	E.L.	+
Panchal, S. et al <sup>52</sup>	0	Bernardi	Bernardi			T	Neural network, heat from current collector tabs included	20 Ah battery	P	2, 4	C		LiFePO <sub>4</sub>
Samba, A; et al <sup>53</sup>	2	Bernardi	Bernardi	Convection Radiation		T	Surface temperature prediction, fewer input parameters with high accuracy	45 Ah cell			C		LiFePO <sub>4</sub>
Shah, et al <sup>54</sup>	0	Reaction	Ohmic	Convection		T	Transient heat generation model with various charge profiles	Test cell shaped as 26650	C				
Walker, et al <sup>55</sup>	3	Bernardi	Bernardi	Conduction Convection Radiation	Chen <sup>36</sup>	T-EC	Using Thermal Desktop to validate battery model for use in spaceflight applications	185 Amp-Hour (Ah) LIB	P	1, 2, 3			
Walker, et al <sup>13</sup>	3	Bernardi	Bernardi	Conduction Convection Radiation	Chen <sup>36</sup>	T-EC	Testing Boston Power Swing 5300 cells and evaluation of Thermal Desktop/SINDA model	Boston Power Swing 5300 Li-ion cells, 300 cell stack	C		C	Liq.	LiCoO <sub>2</sub>

Table 3. Analytical/P2D Models

Author	Dim	Rev. HG	Irr. HG	Ext. B.C.	E.C.	Multi	Novelty	Cells, Batteries	Geo.	C-Rate	-	E.L.	+
Bahiraei, F. et al <sup>22</sup>	P3	Reaction	Ohmic, polarization	Convection (radiation neglected)	Butler-Volmer	T-EC	Simplified 1D EC model to speed computation	4 Ah LiNiCoAlO <sub>2</sub> (NCA)	P	0.5, 1, 2, 4	C		LiNiCoAlO <sub>2</sub>
Basu, S. et al <sup>20</sup>	3	Reaction	Ohmic	Conduction	P2D	T-EC	Liquid coolant for 18650 developed	18650, 6 in series, 5 in parallel	C	0.6, 0.9	C		Li-NCA
Cai, White <sup>21</sup>	1/P 2	Reaction	Overvoltage, Ohmic	Convection	P2D	T-EC	Extending COMSOL Li-ion battery model	Single cell		0.5, 1, 3			
Farag, M et. al. <sup>27</sup>	0	Bernardi	Bernardi		P2D	T-EC	Reduced order multi-physics model capable of predicting cell voltage and core temperature	NCM cell	P	C/52	C		NMC Li[MnNiCo]O <sub>2</sub>
Fu, R, et al <sup>56</sup>	1	Reaction mixing	Ohmic	Convection	Butler-Volmer, Tafel, Nernst	T-EC	Side reaction contributions to SEI thickness integrated into model	LiPb, 15.7 Ah	P		C	LiPF <sub>6</sub>	NMC (Li[MnNiCo]O <sub>2</sub> )
Fuller, T et al <sup>57</sup>	1				P2D	EC	General model for dual insertion cell. Reduced computation time using superposition	Single cell			C		LiMn <sub>2</sub> O <sub>4</sub>

Table 3. Analytical/P2D Models (continued)

Author	Dim	Rev. HG	Irr. HG	Ext. B.C.	E.C.	Multi	Novelty	Cells, Batteries	Geo.	C-Rate	-	E.L.	+
Gerver, R; Meyers, J <sup>58</sup>	1/2/ 3	Reaction	Ohmic		P2D	T-EC	Local state of charge prediction, 3D current distributions using 2D resistor network coupled with 1D EC model	2/5 cell stack	P	5	C		LiFePO <sub>4</sub>
Ghalkhani, M. et al <sup>59</sup>	1/3	Reaction	Ohmic	Convection	Newman	T-EC	Energy density, temperature response, overall heat generation and distribution	10 Ah Tenergy PL78721 96	P	0.8	C		LiNiCo AlO <sub>2</sub>
Gu, W.B.; Wang, C.Y. <sup>37</sup>	1/2/ 3	Bernardi	Bernardi	Convection	Porous electrode	T-EC	Can be applied to most battery systems, thermal energy equation based on first principles	NiMH cell				KOH	
Guo, M; White, R <sup>23</sup>	P2	Reaction	Ohmic	Convection	P2D	T-EC	Reduce computation time via linear approximation method (decouple electrochemical from heat), high charge rate	Electrode Pair	P	5	C		LiNiCo AlO <sub>2</sub> (NCA)
Guo, M., et al <sup>60</sup>	P2/ 3	Volume Average	Ohmic	Convection	P2D	T-EC	Linear approximation, added bus bars to tabs	3 Li-ion cells in series	P	1, 3, 5			
Jeon, D.H. <sup>61</sup>	1/P 2/3	Bernardi	Bernardi		P2D	T-EC	Heat contributions at various C-rates using commercial software	18650	C	0.5, 1, 2	C	LiPF <sub>6</sub>	LiCoO <sub>2</sub>

Table 3. Analytical/P2D Models (continued)

Author	Dim	Rev. HG	Irr. HG	Ext. B.C.	E.C.	Multi	Novelty	Cells, Batteries	Geo.	C-Rate	-	E.L.	+
Jiang, F., et. al. <sup>62</sup>	3	Reaction (side reactions ignored)	Ohmic	Convection	P2D	T-EC	Considers thermal contact resistance			1, 3, 5	C	LiPF <sub>6</sub>	LiFePO <sub>4</sub>
Kumaresan, K, et al <sup>63</sup>	0	Gu	Gu	Gu	P2D	T-EC	Predict discharge performance at various temperatures	1.656 Ah pouch	P	1/33, 0.5, 1	C	LiPF <sub>6</sub>	LiCoO <sub>2</sub>
Kwon, K.H. et al <sup>44</sup>	2					EC	Effect of aspect ratio and electrode placement on potential and current density distribution	5 Ah (VK Corp.)	P	1, 2, 3, 5, 8, 10	C		LiMn <sub>2</sub> O <sub>4</sub>
Lee, C.H.; Bae, S; Jang, M <sup>64</sup>	0	Reaction	Ohmic	Convection	Butler-Volmer, Dahn		Ohmic heating model including short circuit current	3.43, 2.43, 2.5 Ah	P/C	0.2, 0.5, 1			
Lee, K et al <sup>25</sup>	3	MSMD	MSMD	MSMD	MSMD	T-EC	Wound potential pair continuum (WPPC) developed	20 Ah large format cylinder	C				
Li, X, et al <sup>65</sup>	0/3	Reaction mixing	Ohmic	Convection	Fick's Law, Butler-Volmer	T-EC	Reduced order model for use in BMS	Li-polymer pouch	P	1, 2, 5	C		LiMn <sub>2</sub> O <sub>4</sub>
Wang, et al <sup>66</sup>	3D				Nernst-Planck, Butler-Volmer	EC	FE analysis of 3D porous cathode, Li diffusivity, contact resistances	Lithium polymer cell			C	PEO1 2-LiCl O <sub>4</sub>	LiMn <sub>2</sub> O <sub>4</sub>

Table 3. Analytical/P2D Models (continued)

Author	Dim	Rev. HG	Irr. HG	Ext. B.C.	E.C.	Multi	Novelty	Cells, Batteries	Geo.	C-Rate	-	E.L.	+
Ye, Y., et al. <sup>67</sup>	0	Reaction (side reactions ignored)	Ohmic, polarization	Convection	Doyle, Butler-Volmer	T-EC	Li-ion concentration gradients affected by temperature, experimental validation	11.5 Ah battery		0.2, 0.5, 1, 2	C	PC/E C/D MC	LiMn <sub>2</sub> O <sub>4</sub>
Zhang, X. <sup>68</sup>	0/1	Reaction	Ohmic, polarization	Convection	Newman, Butler-Volmer	T-EC	Finds that Ohmic heat is the largest contribution to heat generation	26650 Single cell	C	0.5, 1, 1.7	C	LiPF <sub>6</sub> (PC/E C/D MC)	LiMn <sub>2</sub> O <sub>4</sub>
Zhu, C., et al. <sup>69</sup>	0	Reaction	Ohmic	Convection (natural and forced)	P2D	T-EC	Interstitial cooling channels, heat transfer between adjacent cells	144V/6 Ah pack	P	1, 5	C	LiPF <sub>6</sub>	LiMn <sub>2</sub> O <sub>4</sub>

Table 4. Thermal Runaway Models

Author	Dim.	Rev. HG	Irr. HG	Ext. B.C.	E.C.	Multi	Novelty	Cells, Batteries	Geo.	TR	C-Rate	-	E.L	+
Al-Hallaj, et al <sup>70</sup>	0/1	Reaction	Overvoltage	Convection		T	Radial temperature profile simulation	Sony US 18650, 10/100 Ah	C	Discharge rate, internal short	1/2, 1/3, 1/6, 1			
Chiu, K.C., et al <sup>31</sup>	3	Bernardi	Bernardi		P2D	T-EC	Mass and charge transfer implemented for short-circuited Li-ion cell, considers entropic heating due to nail penetration	ITRI 5.25 Ah LMO	P	Nail penetration, internal short	1, 2, 3	C		Li Mn <sub>2</sub> O <sub>4</sub>
Chen, Y; Evans J <sup>36</sup>	3	Bernardi	Bernardi	Convection Radiation	Shepherd	T-EC	Heat generation and transport during cycles (SFUDS), choose insulating materials, cooling channel configurations	Sony 20500 900 mAh, prismatic cell	P/C	Overheat	0.3, 0.45, 0.9, 1.8	C		LiCoO <sub>2</sub>
Chen, M. et al <sup>71</sup>	0/1/3	Reaction	Ohmic	Convection Radiation	P2D	T-EC	Thermal decomposition reactions, isothermal battery (neglects hot spots during TR)	50 Ah 1/8th Lithium titanate cell	C	Overheat, C2C Propagation	0.1, 0.5, 1, 1.5	Li Ti		LiNiCoMnO

Table 4. Thermal Runaway Models (continued)

Author	Dim.	Rev. HG	Irr. HG	Ext. B.C.	E.C.	Multi	Novelty	Cells, Batteries	Geo.	TR	C-Rate	-	E.L	+
Coman, et al <sup>12</sup>	0	ODE	ODE	Convection Radiation	Empirical (Arrhenius)	T-EC	Considers ejecta, J-T effect during TR	18650 LCO	C	Overheat/Overpressure		C		LiCoO <sub>2</sub>
Guo, G, et al <sup>72</sup>	3	Bernardi	Bernardi	Convection Radiation		T-EC	3D Thermal Abuse model (oven test)	VLP 50/62/10 0S-Fe (3.2V/55 Ah)	P	Overheat	1/3, 1	C		LiFePO <sub>4</sub>
Hatchard, et al <sup>18</sup>	0/1	Reaction		Convection Radiation	Empirical (Arrhenius)	T-EC	Introduced cathode decomposition	18650 1.6 Ah, LiCoO <sub>2</sub> /graphite cells	P/C	Overheat		C		LiCoO <sub>2</sub>
Kim G.H., et al <sup>28</sup>	1/3	Reaction	Ohmic	Convection Radiation	Empirical (Arrhenius)	T-EC	Hatchard was reproduced, then it was extended to 3 dimensions, local hot spot propagation	D50H90	C	Overheat, Internal short circuit neglected		C	LiPF <sub>6</sub>	LiCoO <sub>2</sub>
Larsson, F., et al. <sup>73</sup>	3D			Convection Radiation		T	C2C propagation, fire impingement study	EiG ePLB-F007A, 7 Ah 5 cell stack	P	C2C, Cell swelling neglected		C		LiFePO <sub>4</sub>

Table 4. Thermal Runaway Models (continued)

Author	Dim.	Rev. HG	Irr. HG	Ext. B.C.	E.C.	Multi	Novelty	Cells, Batteries	Geo.	TR	C-Rate	-	E.L	+
Liang, G., et al, <sup>29</sup>	3D	Reaction, side reactions	Ohmic, polarization	Convection Radiation	Hatchard	T-EC	Method for determining short-circuit area equivalent resistance	5.25, 2.5, 5, 3.2, 100 Ah	P	Internal short, nail penetration				
Liu, B., et al. <sup>34</sup>	1/2	Reaction	Ohmic	Convection Radiation	Newman	T-EC	Mechanical deformation TR model, short circuit	Single 18650 cell	C	Mechanical deformation, short circuit	0.3, 1	C	LiP F <sub>6</sub>	LiC oO <sub>2</sub>
Ren, D., et al. <sup>74</sup>	0				Energy Balance	T-EC	Overcharge thermal runaway model	40 Ah Li-ion	P	Overcharge	0.33, 0.5, 1	C		Li Mn <sub>2</sub> O <sub>4</sub>
Yayathi, S; Walker, W <sup>75</sup>	0	ODE	ODE	Quasi-adiabatic	Empirical (Arrhenius)	T-EC	Calorimeter testing thermal runaway, verifying batteries for spaceflight applications	Power Swing 5300, Samsung 18650-26F, MoliCel 18650-J	C	Overheat				
Zhang, C., et al <sup>33</sup>	3		Ohmic		Fuller	T-EC	Mechanical deformation model coupled with internal short circuit model	740 mAh pouch cell	P	Crush		C		LiC oO <sub>2</sub>

Table 4. Thermal Runaway Models (continued)

Author	Dim.	Rev. HG	Irr. HG	Ext. B.C.	E.C.	Multi	Novelty	Cells, Batteries	Geo.	TR	C-Rate	-	E.L	+
Zhao, R., Liu, J., Junjie, G. <sup>32</sup>	3	Reaction (entropy heat ignored)	Ohmic	Convection Radiation	Doyle	T-EC	External and Internal short circuit (nail penetration), interstitial material investigation, Joule heating from nail added	4S1P battery packs and others, 6 total, 1.5 and 5 Ah	P	Nail penetrati- on	1	C		LiC oO <sub>2</sub>
Zhao, W, et al <sup>76</sup>	3	Reaction	Ohmic		Luo/ Wang	T-EC	Considers nail diameter, nail thermal conductivity, shorting resistance	5 Ah single cell	P	Internal short, nail penetrati- on		C		LiC oNi Mn O <sub>2</sub>

Table 5. Battery Management System (BMS) Models

Author	Dim.	Rev. HG	Irr. HG	Ext. B.C.	E.C.	Multi	Novelty	Cells, Batteries	Geo.	C-Rate	-	E.L.	+
Bahiraei, F. et al <sup>22</sup>	P3	Reaction	Ohmic, polarization	Convection (radiation neglected)	Butler-Volmer	T-EC	Simplified 1D EC model to speed computation	4Ah LiNiCoAlO <sub>2</sub> (NCA)	P	0.5, 1, 2, 4	C		LiNiCoAlO <sub>2</sub>
Chacko; Chung <sup>43</sup>	3	Bernardi <sup>15</sup>	Bernardi	Convection	Kwon <sup>44</sup> PDE	T-EC	Modified Newman <sup>38</sup> to estimate current density, Seebeck effect, during both charge and discharge	20 Ah single cell	P	0.5, 1.2, 3, 5	C		Li[NiMnCo]O <sub>2</sub>
Damay, et al <sup>46</sup>	0	Reaction	Ohmic	Insulation, Convection		T/E	Uses equivalent circuit for use in BMS microcontroller	40 Ah battery	P	0.5, 2	C		LiFePO <sub>4</sub>
Farag, M et. al. <sup>27</sup>	0	Bernardi	Bernardi		P2D	T-EC	Reduced order multi-physics model capable of predicting cell voltage and core temperature	NCM cell	P	C/52	C		NMC Li[MnNiCo]O <sub>2</sub>

Table 5. Battery Management System (BMS) Models (continued)

Author	Dim.	Rev. HG	Irr. HG	Ext. B.C.	E.C.	Multi	Novelty	Cells, Batteries	Geo.	C-Rate	-	E.L.	+
Forgez, et al <sup>47</sup>	0	Thomas <sup>42</sup>	Thomas	HT w/ surround.		T	Simplified thermal model, estimate internal isothermal temperature for use in BMS	26650 single cell	C	6	C		LiFePO <sub>4</sub>
Li, X, et al <sup>65</sup>	0/3	Reaction mixing	Ohmic	Convection	Fick's Law, Butler-Volmer	T-EC	Reduced order model for use in BMS	Pouch type Li-polymer single cell	P	1, 2, 5	C		LiMn <sub>2</sub> O <sub>4</sub>
Nieto, N, et al <sup>51</sup>	0	Bernardi	Bernardi	Convection Radiation		T	Faster discharge rates considered, internal resistance is used to measure overpotential	Tenergy 30123 10.5 Ah cell	P	1, 3, 5			

Table 6. All models (alphabetical order)

Author	Dim.	Rev. HG	Irr. HG	Ext. B.C.	E.C.	Multi	Novelty	Cells, Batteries	Geo.	C-Rate	-	E.L.	+
Al-Hallaj, et al <sup>70</sup>	0/1	Reaction	Overvoltage	Convection		T	Radial temperature profile simulation	Sony US 18650, 10/100 Ah	C	1/2, 1/3, 1/6, 1			
Bahiraeei, F. et al <sup>22</sup>	P3	Reaction	Ohmic, polarization	Convection (radiation neglected)	Butler-Volmer	T-EC	Simplified 1D EC model to speed computation	4Ah LiNiCo AlO <sub>2</sub> (NCA)	P	0.5, 1, 2, 4	C		LiNiCo AlO <sub>2</sub>
Basu, S. et al <sup>20</sup>	3	Reaction	Ohmic	Conduction	P2D	T-EC	Liquid coolant for 18650 developed	18650, 6 in series, 5 in parallel	C	0.6, 0.9	C		Li-NCA
Cai; White <sup>21</sup>	1/P2	Reaction	Overvoltage, Ohmic	Convection	P2D	T-EC	Extending COMSOL Li-ion battery model	Single cell		0.5, 1, 3			
Chacko; Chung <sup>43</sup>	3	Bernardi	Bernardi	Convection	Kwon <sup>44</sup> PDE	T-EC	Modified Newman <sup>38</sup> to estimate current density, Seebeck effect, during both charge and discharge	20 Ah single cell	P	0.5, 1.2, 3, 5	C		Li[NiMnCo]O <sub>2</sub>
Chen, M. et al <sup>71</sup>	0/1/3	Reaction	Ohmic	Convection Radiation	P2D	T-EC	Thermal decomposition reactions, isothermal battery (neglects hot spots during TR)	50 Ah 1/8th Lithium titanate cell	C	0.1, 0.5, 1, 1.5	LiTi		LiNiCo MnO

Table 6. All models (continued)

Author	Dim.	Rev. HG	Irr. HG	Ext. B.C.	E.C.	Multi	Novelty	Cells, Batteries	Geo.	C-Rate	-	E.L.	+
Chen, S.C., et al <sup>45</sup>	2	Bernardi	Bernardi	Convection (natural, forced parallel & cross flow), Radiation		T/E	Spiral geometry model developed (instead of concentric rings like Hatchard <sup>18</sup> ), radial temperature profile	0.08, 2.16, 10, 27.44, 58.32, 106.48 Ah	C	1, 3	C	Liq	LiCoO <sub>2</sub>
Chen, S.C., et al <sup>36</sup>	1/2/3	Bernardi	Bernardi	Convection (natural, forced), Radiation		T/E	Simplified thermal model with fast computation speed	185.3 Ah Li-ion battery	P	0.2, 1, 2, 3	C	Liq	LiCoO <sub>2</sub>
Chen, Y; Evans J <sup>36</sup>	3	Bernardi	Bernardi	Convection Radiation	Shepherd	T-EC	Heat generation and transport during cycles (SFUDS), choose insulating materials, cooling channel configurations	Sony 20500 900 mAh, prismatic cell	P/C	0.3, 0.45, 0.9, 1.8	C		LiCoO <sub>2</sub>
Chiu, K.C., et al <sup>31</sup>	3	Bernardi	Bernardi		P2D	T-EC	Mass and charge transfer implemented for short-circuited Li-ion cell, considers entropic heating due to nail penetration	ITRI 5.25 Ah LMO	P	1, 2, 3	C		LiMn <sub>2</sub> O <sub>4</sub>

Table 6. All models (continued)

Author	Dim.	Rev. HG	Irr. HG	Ext. B.C.	E.C.	Multi	Novelty	Cells, Batteries	Geo.	C-Rate	-	E.L.	+
Coman, et al <sup>12</sup>	0	ODE	ODE	Convection Radiation	Empirical	T-EC	Considers ejecta, J-T effect during TR	18650 LCO	C		C		LiCoO <sub>2</sub>
Damay, et al <sup>46</sup>	0	Reaction	Ohmic	Insulation, Convection		T/E	Uses equivalent circuit for use in BMS microcontroller	40 Ah battery	P	0.5, 2	C		LiFePO <sub>4</sub>
Farag, M et. al. <sup>27</sup>	0	Bernardi	Bernardi		P2D	T-EC	Reduced order multi-physics model capable of predicting cell voltage and core temperature	NCM cell	P	C/52	C		NMC Li[MnNiCo]O <sub>2</sub>
Forgez, et al <sup>47</sup>	0	Thomas <sup>4</sup> <sub>2</sub>	Thomas	HT w/ surround.		T	Simplified thermal model, estimate internal isothermal temperature for use in BMS	26650 single cell	C	6	C		LiFePO <sub>4</sub>
Fu, R, et al <sup>56</sup>	1	Reaction mixing	Ohmic	Convection	Butler-Volmer, Tafel, Nernst	T-EC	Side reaction contributions to SEI thickness integrated into model	LiPb, 15.7 Ah	P		C	LiP F <sub>6</sub>	NMC (Li[MnNiCo]O <sub>2</sub> )
Fuller, T et al <sup>57</sup>	1				P2D	EC	General model for dual insertion cell. Reduced computation time using superposition	Single cell			C		LiMn <sub>2</sub> O <sub>4</sub>

Table 6. All models (continued)

Author	Dim.	Rev. HG	Irr. HG	Ext. B.C.	E.C.	Multi	Novelty	Cells, Batteries	Geo.	C-Rate	-	E.L.	+
Gerver, R; Meyers, J <sup>58</sup>	1/2/3	Reaction	Ohmic		P2D	T-EC	Local state of charge prediction, 3D current distributions using 2D resistor network coupled with 1D EC model	2/5 cell stack	P	5	C		LiFePO <sub>4</sub>
Ghalkhani, M. et al <sup>59</sup>	1/3	Reaction	Ohmic	Convection	Newman	T-EC	Energy density, temperature response, overall heat generation and distribution	10 Ah Tenergy PL78721 96	P	0.8	C		LiNiCo AlO <sub>2</sub>
Gu, W.B.; Wang, C.Y. <sup>37</sup>	1/2/3	Bernardi	Bernardi	Convection	Porous electrode	T-EC	Can be applied to most battery systems, thermal energy equation based on first principles	NiMH cell				KO H	
Gumussu, et al <sup>48</sup>	3	Bernardi	Bernardi	Convection		T/E	3D CFD natural convection analysis (external)	Panasonic NCR1865 0B	C	0.5, 1.0, 1.5			
Guo, G, et al <sup>72</sup>	3	Bernardi	Bernardi	Convection Radiation		T-EC	3D Thermal Abuse model (oven test)	VLP 50/62/10 0S-Fe (3.2V/55 Ah)	P	1/3, 1	C		LiFePO <sub>4</sub>

Table 6. All models (continued)

Author	Dim.	Rev. HG	Irr. HG	Ext. B.C.	E.C.	Multi	Novelty	Cells, Batteries	Geo.	C-Rate	-	E.L.	+
Guo, M; White, R <sup>23</sup>	P2	Reaction	Ohmic	Convection	P2D	T-EC	Reduce computation time via linear approximation method (decouple electrochemical from heat), high charge rate	Electrode Pair	P	5	C		LiNiCoAlO <sub>2</sub> (NCA)
Guo, M., et al <sup>60</sup>	P2/3	Volume Average	Ohmic	Convection	P2D	T-EC	Linear approximation, added bus bars to tabs	3 Li-ion cells in series	P	1, 3, 5			
Hatchard, et al <sup>18</sup>	0/1	Reaction		Convection Radiation	Empirical (Arrhenius)	T-EC	Introduced cathode decomposition	18650 1.6 Ah, LiCoO <sub>2</sub> /graphite cells	P/C		C		LiCoO <sub>2</sub>
Jeon, D.H. <sup>61</sup>	1/P2/3	Bernardi	Bernardi		P2D	T-EC	Heat contributions at various C-rates using commercial software	18650	C	0.5, 1, 2	C	LiP F <sub>6</sub>	LiCoO <sub>2</sub>
Jeon; Baek <sup>49</sup>	3	Bernardi	Bernardi	Convection	Energy Balance	T/E	Analyzes contributions to entropy change from rev. and irr. sources at various C-rates	1.5 Ah Sony 18650 LiCoO <sub>2</sub> /C	C	0.5, 1, 2, 3, 4, 5	C		LiCoO <sub>2</sub>

Table 6. All models (continued)

Author	Dim.	Rev. HG	Irr. HG	Ext. B.C.	E.C.	Multi	Novelty	Cells, Batteries	Geo.	C-Rate	-	E.L.	+
Jiang, F., et al. <sup>62</sup>	3	Reaction (side reactions ignored)	Ohmic	Convection	P2D	T-EC	Considers thermal contact resistance			1, 3, 5	C	LiP F <sub>6</sub>	LiFePO <sub>4</sub>
Kim G.H., et al <sup>28</sup>	1/3	Reaction	Ohmic	Convection Radiation	Empirical (Arrhenius)	T-EC	Hatchard was reproduced, then it was extended to 3 dimensions, local hot spot propagation	D50H90	C		C	LiP F <sub>6</sub>	LiCoO <sub>2</sub>
Kim, U; Yi, J, et al <sup>50</sup>	2	Bernardi	Bernardi	Convection	Kwon PDE	T-EC	Effect of charge conditions on thermal behavior	14.6 Ah LG Chem.	P	1, 3, 5	C		LiMn <sub>2</sub> O <sub>4</sub>
Kumaresan, K, et al <sup>63</sup>	0	Gu	Gu	Gu	P2D	T-EC	Predict discharge performance at various temperatures	1.656 Ah pouch	P	1/33, 0.5, 1	C	LiP F <sub>6</sub>	LiCoO <sub>2</sub>
Kwon, K.H. et al <sup>44</sup>	2					EC	Effect of aspect ratio and electrode placement on potential and current density distribution	5 Ah (VK Corp.)	P	1, 2, 3, 5, 8, 10	C		LiMn <sub>2</sub> O <sub>4</sub>
Larsson, F., et al. <sup>73</sup>	3D			Convection Radiation		T	C2C propagation, fire impingement study	EiG ePLB-F007A, 7 Ah 5 cell stack	P		C		LiFePO <sub>4</sub>

Table 6. All models (continued)

Author	Dim.	Rev. HG	Irr. HG	Ext. B.C.	E.C.	Multi	Novelty	Cells, Batteries	Geo.	C-Rate	-	E.L.	+
Lee, C.H.;Bae, S.;Jang, M <sup>64</sup>	0	Reaction	Ohmic	Convection	Butler-Volmer, Dahn		Ohmic heating model including short circuit current	3.43, 2.43, 2.5 Ah	P/C	0.2, 0.5, 1			
Lee, K et al <sup>25</sup>	3	MSMD	MSMD	MSMD	MSMD	T-EC	Wound potential pair continuum (WPPC) developed	20 Ah large format cylinder	C				
Li, X, et al <sup>65</sup>	0/3	Reaction mixing	Ohmic	Convection	Fick's Law, Butler-Volmer	T-EC	Reduced order model for use in BMS	Li-polymer pouch	P	1, 2, 5	C		LiMn <sub>2</sub> O <sub>4</sub>
Liang, G., et, al, <sup>29</sup>	3D	Reaction, side reactions	Ohmic, polarization	Convection Radiation	Hatchard	T-EC	Method for determining short-circuit area equivalent resistance	5.25, 2.5, 5, 3.2, 100 Ah	P				
Liu, B., et. al. <sup>34</sup>	1/2	Reaction	Ohmic	Convection Radiation	Newman	T-EC	Mechanical deformation TR model, short circuit	Single 18650 cell	C	0.3, 1	C	LiP F <sub>6</sub>	LiCoO <sub>2</sub>
Nieto, N, et al <sup>51</sup>	0	Bernardi	Bernardi	Convection Radiation		T	Faster discharge rates considered, internal resistance is used to measure overpotential	Tenergy 30123 10.5 Ah cell	P	1, 3, 5			

Table 6. All models (continued)

Author	Dim.	Rev. HG	Irr. HG	Ext. B.C.	E.C.	Multi	Novelty	Cells, Batteries	Geo.	C-Rate	-	E.L.	+
Panchal, S. et al <sup>52</sup>	0	Bernardi	Bernardi			T	Neural network, heat from current collector tabs included	20 Ah battery	P	2, 4	C		LiFePO <sub>4</sub>
Ren, D., et al. <sup>74</sup>	0				Energy Balance	T-EC	Overcharge thermal runaway model	40 Ah Li-ion	P	0.33, 0.5, 1	C		LiMn <sub>2</sub> O <sub>4</sub>
Samba, A; et al <sup>53</sup>	2	Bernardi	Bernardi	Convection Radiation		T	Surface temperature prediction, fewer input parameters with high accuracy	45 Ah cell			C		LiFePO <sub>4</sub>
Shah, et al <sup>54</sup>	0	Reaction	Ohmic	Convection		T	Transient heat generation model with various charge profiles	Test cell shaped as 26650	C				
Tanaka, N., et al. <sup>77</sup>	1			Convection Radiation	Safari model	EC	DSC simulation predicting thermal runaway	26650 cell	C				
Walker, et al <sup>55</sup>	3	Bernardi	Bernardi	Conduction Convection Radiation	Chen <sup>36</sup>	T-EC	Using Thermal Desktop to validate battery model for use in spaceflight applications	185 Amp-Hour (Ah) LIB	P	1, 2, 3			

Table 6. All models (continued)

Author	Dim.	Rev. HG	Irr. HG	Ext. B.C.	E.C.	Multi	Novelty	Cells, Batteries	Geo.	C-Rate	-	E.L.	+
Walker, et al <sup>13</sup>	3	Bernardi	Bernardi	Conduction Convection Radiation	Chen <sup>36</sup>	T-EC	Testing Boston Powser Swing 5300 cells and evaluation of Thermal Desktop/SINDA model	Boston Power Swing 5300 Li-ion cells, 300 cell stack	C		C	Liq.	LiCoO <sub>2</sub>
Wang, et al <sup>66</sup>	3D				Nernst-Planck, Butler-Volmer	EC	FE analysis of 3D porous cathode, Li diffusivity, contact resistances	Lithium polymer cell			C	PEO 12-LiCl O <sub>4</sub>	LiMn <sub>2</sub> O <sub>4</sub>
Yayathi, S; Walker, W <sup>75</sup>	0	ODE	ODE	Quasi-adiabatic	Empirical (Arrhenius)	T-EC	Calorimeter testing thermal runaway, verifying batteries for spaceflight applications	Power Swing 5300, Samsung 18650-26F, MoliCel 18650-J	C				
Ye, Y., et al <sup>67</sup>	0	Reaction (side reactions ignored)	Ohmic, polarization	Convection	Doyle, Butler-Volmer	T-EC	Li-ion concentration gradients affected by temperature, experimental validation	11.5 Ah battery		0.2, 0.5, 1, 2	C	PC/EC/DMC	LiMn <sub>2</sub> O <sub>4</sub>
Zhang, C., et al <sup>33</sup>	3		Ohmic		Fuller	T-EC	Mechanical deformation model coupled with internal short circuit model	740 mAh pouch cell	P		C		LiCoO <sub>2</sub>

Table 6. All models (continued)

Author	Dim.	Rev. HG	Irr. HG	Ext. B.C.	E.C.	Multi	Novelty	Cells, Batteries	Geo.	C-Rate	-	E.L.	+
Zhang, X. <sup>68</sup>	0/1	Reaction	Ohmic, polarization	Convection	Newman, Butler-Volmer	T-EC	Finds that Ohmic heat is the largest contribution to heat generation	26650 Single cell	C	0.5, 1, 1.7	C	LiP F <sub>6</sub> (PC/EC/DMC)	LiMn <sub>2</sub> O <sub>4</sub>
Zhao, R., Liu, J., Junjie, G. <sup>32</sup>	3	Reaction (entropy heat ignored)	Ohmic	Convection Radiation	Doyle	T-EC	External and Internal short circuit (nail penetration), interstitial material investigation, Joule heating from nail added	4S1P battery packs and others, 6 total, 1.5 and 5 Ah	P	1	C		LiCoO <sub>2</sub>
Zhao, W, et al. <sup>76</sup>	3	Reaction	Ohmic		Luo/Wang	T-EC	Considers nail diameter, nail thermal conductivity, shorting resistance	5 Ah single cell	P		C		LiCoNi MnO <sub>2</sub>
Zhu, C., et al. <sup>69</sup>	0	Reaction	Ohmic	Convection (natural and forced)	P2D	T-EC	Interstitial cooling channels, heat transfer between adjacent cells	144V/6 Ah pack	P	1, 5	C	LiP F <sub>6</sub>	LiMn <sub>2</sub> O <sub>4</sub>

## Chapter 4. Application

Researchers and engineers at the National Aeronautics and Space Administration (NASA) choose commercially available cells for their designs when developing spacesuits, or power tools used by astronauts during Extravehicular Activities (EVA) (also known as spacewalks), or the batteries that power the International Space Station (ISS), or robotic humanoid helpers.<sup>13</sup> This implies that although battery chemistry may be an important factor for determining a particular cell's compatibility within a system, designers are limited to what the market offers and therefore may not be so concerned with battery chemistry and more concerned with cell performance. In which case, a designer would make use of Table 1, which lists empirical heat generation models that better lend themselves to performance modeling as compared to electrochemical models, not to mention they are typically faster to solve. Additionally, each table lists the manufacturer and model of cells used either in the model or in experiment to verify the model.

Models that investigate passive or active thermal management are listed in Table 1 and can be found by using the External Boundary Condition (Ext. B.C.) column, or the Novelty column, if thermal management is necessary on the exterior of a cell. Some analytical models, listed in Table 2, investigate thermal management as well. Table 4 would also become useful, which lists thermal runaway models, some of which also investigate interstitial insulation, cooling channels, and heaters. It is of the utmost importance to avoid thermal runaway, most especially during crewed missions, so the risk must be well understood.

If high charge/discharge rates are a concern, this author has found that most models are generally accurate at low C-rates, however, begin to lose significant accuracy when simulating rates of 5 C and higher. Therefore, if certain charge or discharge rates need to be simulated, each table lists the C-rate used for each model (if provided or applicable), and those listed with rates greater than 5 C have had varying degrees of success limiting the error in their simulations. Kwon et. al.<sup>44</sup> reports good agreement with experiment at rates up to 10 C.

The ISS contains a large number of high-power batteries and they all must be actively managed, which would make Table 5 especially useful as it lists models that are fast and accurate enough for real-time battery management systems.

## Chapter 5. Conclusions and Future Work

### 5.1 Conclusions

Various Li-ion cell modeling techniques were described and presented in detail. The summary tables in Chapter 3 will allow researchers to identify which thermal runaway models and triggering mechanisms have been modeled. This paper will allow others to develop tools for battery safety, select and design insulative or interstitial materials for thermal management, and to choose and implement models for battery management systems. The tables can be used to identify other gaps in knowledge, for instance, only a single model was found to simulate thermal runaway induced by overcharging.

### 5.2 Future Work

To the best of the author's knowledge, the information collected here can is not available in a single resource elsewhere. Chapter 2 can be expanded to include other modeling techniques still, such as the Frank-Kamenetskii or Semenov models, and the tables in Chapter 3 can be expanded by adding more models and more detail. By using the tables, models that accurately and quickly predict cell performance can be improved by comparing computational costs for each modeling approach.

## References

1. Tarascon, J. M. & Armand, M. B. Issues and challenges facing rechargeable lithium batteries. *Nature* **414**, 359–367 (2001).
2. Moura, S. J., Siegel, J. B., Siegel, D. J., Fathy, H. K. & Stefanopoulou, A. G. Education on vehicle electrification: Battery systems, fuel cells, and hydrogen. *2010 IEEE Veh. Power Propuls. Conf. VPPC 2010* (2010).  
doi:10.1109/VPPC.2010.5729150
3. Eisenstein, P. GM Is Going All Electric, Will Ditch Gas- and Diesel-Powered Cars. (2017). Available at: <https://www.nbcnews.com/business/autos/gm-going-all-electric-will-ditch-gas-diesel-powered-cars-n806806>.
4. Arar, J. I. New Directions: The electric car and carbon emissions in the US. *Atmos. Environ.* **44**, 733–734 (2010).
5. Lisbona, D. & Snee, T. A review of hazards associated with primary lithium and lithium-ion batteries. *Process Saf. Environ. Prot.* **89**, 434–442 (2011).
6. Feng, X., Lu, L., Ouyang, M., Li, J. & He, X. A 3D thermal runaway propagation model for a large format lithium ion battery module. *Energy* **115**, 194–208 (2016).
7. Byford, S. Samsung recalls Galaxy Note 7 worldwide due to exploding battery fears. (2016). Available at:  
<https://www.theverge.com/2016/9/2/12767670/samsung-galaxy-note-7-recall-fire-risk>. (Accessed: 24th September 2018)
8. Van Noorden, R. A better battery. *Nature* **507**, 26 (2014).
9. Kubota, K., Dahbi, M., Hosaka, T., Kumakura, S. & Komaba, S. Towards K-Ion and Na-Ion Batteries as “Beyond Li-Ion”. *Chem. Rec.* **18**, 459–479 (2018).

10. Bandhauer, T. M., Garimella, S. & Fuller, T. F. A Critical Review of Thermal Issues in Lithium-Ion Batteries. *J. Electrochem. Soc.* **158**, R1 (2011).
11. Maleki, H. Thermal Properties of Lithium-Ion Battery and Components. *J. Electrochem. Soc.* **146**, 947 (1999).
12. Coman, P. T., Rayman, S. & White, R. E. A lumped model of venting during thermal runaway in a cylindrical Lithium Cobalt Oxide lithium-ion cell. *J. Power Sources* **307**, 56–62 (2016).
13. Walker, W., Yayathi, S., Shaw, J. & Ardebili, H. Thermo-electrochemical evaluation of lithium-ion batteries for space applications. *J. Power Sources* **298**, 217–227 (2015).
14. Sherfey, J. M. & Brenner, A. Electrochemical Calorimetry. *J. Electrochem. Soc.* **105**, 665 (1958).
15. Bernardi, D. A General Energy Balance for Battery Systems. *J. Electrochem. Soc.* **132**, 5 (1985).
16. Richard, M. N. & Dahn, J. R. Accelerating Rate Calorimetry Study on the Thermal Stability of Lithium Intercalated Graphite in Electrolyte. II. Modeling the Results and Predicting Differential Scanning Calorimeter Curves. *J. Electrochem. Soc.* **146**, 2078 (1999).
17. Coman, P. T., Darcy, E. C., Veje, C. T. & White, R. E. Modelling Li-Ion Cell Thermal Runaway Triggered by an Internal Short Circuit Device Using an Efficiency Factor and Arrhenius Formulations. *J. Electrochem. Soc.* **164**, A587–A593 (2017).

18. Hatchard, T. D., MacNeil, D. D., Basu, A. & Dahn, J. R. Thermal Model of Cylindrical and Prismatic Lithium-Ion Cells. *J. Electrochem. Soc.* **148**, A755 (2001).
19. Doyle, M. Modeling of Galvanostatic Charge and Discharge of the Lithium/Polymer/Insertion Cell. *J. Electrochem. Soc.* **140**, 1526 (1993).
20. Basu, S., Hariharan, K., Kolake, S., Song, T., Sohn, D.K., Yeo, T. Coupled electrochemical thermal modelling of a novel Li-ion battery pack thermal management system. *Appl. Energy* **181**, 1–13 (2016).
21. Cai, L. & White, R. E. Mathematical Modeling of a Lithium Ion Battery with Thermal Effects in COMSOL Inc. Multiphysics (MP) Software. *J. Power Sources* **196**, 5985–5989 (2011).
22. Bahiraei, F., Ghalkhani, M., Fartaj, A. & Nazri, G. A. A pseudo 3D electrochemical-thermal modeling and analysis of a lithium-ion battery for electric vehicle thermal management applications. *Appl. Therm. Eng.* **125**, 904–918 (2017).
23. Guo, M., White, R. E. & Kim, G. H. A distributed thermal model for a Li-ion electrode plate pair. *J. Power Sources* **221**, 334–344 (2013).
24. Kim, G.-H., Smith, K., Lee, K.-J., Santhanagopalan, S. & Pesaran, A. Multi-Domain Modeling of Lithium-Ion Batteries Encompassing Multi-Physics in Varied Length Scales. *J. Electrochem. Soc.* **158**, A955 (2011).
25. Lee, K. J., Smith, K., Pesaran, A. & Kim, G. H. Three dimensional thermal-, electrical-, and electrochemical-coupled model for cylindrical wound large format lithium-ion batteries. *J. Power Sources* **241**, 20–32 (2013).

26. Guo, M., Kim, G. H. & White, R. E. A three-dimensional multi-physics model for a Li-ion battery. *J. Power Sources* **240**, 80–94 (2013).
27. Farag, M., Sweity, H., Fleckenstein, M. & Habibi, S. Combined electrochemical, heat generation, and thermal model for large prismatic lithium-ion batteries in real-time applications. *J. Power Sources* **360**, 618–633 (2017).
28. Kim, G.-H., Pesaran, A. & Spotnitz, R. A Three-Dimensional Thermal Abuse Model for Lithium-Ion Cells. *J. Power Sources* **170**, 476–489 (2007).
29. Liang, G., Zhang, Y., Han, Q., Liu, Z., Jiang, Z., Tian, S. A novel 3D-layered electrochemical-thermal coupled model strategy for the nail-penetration process simulation. *J. Power Sources* **342**, 836–845 (2017).
30. Feng, X., He, X., Ouyang, M., Lu, L., Wu, P., Kulp, C., Prasser, S. Thermal runaway propagation model for designing a safer battery pack with 25Ah LiNixCoyMnzO2large format lithium ion battery. *Appl. Energy* **154**, 74–91 (2015).
31. Chiu, K. C., Lin, C. H., Yeh, S. F., Lin, Y. H. & Chen, K. C. An electrochemical modeling of lithium-ion battery nail penetration. *J. Power Sources* **251**, 254–263 (2014).
32. Zhao, R., Liu, J. & Gu, J. Simulation and experimental study on lithium ion battery short circuit. *Appl. Energy* **173**, 29–39 (2016).
33. Zhang, C., Santhanagopalan, S., Sprague, M. A. & Pesaran, A. A. Coupled mechanical-electrical-thermal modeling for short-circuit prediction in a lithium-ion cell under mechanical abuse. *J. Power Sources* **290**, 102–113 (2015).

34. Liu, B., Zhao, H., Yu, H., Li, J. & Xu, J. Multiphysics computational framework for cylindrical lithium-ion batteries under mechanical abusive loading. *Electrochim. Acta* **256**, 172–184 (2017).
35. Shah, K., Chalise, D. & Jain, A. Experimental and theoretical analysis of a method to predict thermal runaway in Li-ion cells. *J. Power Sources* **330**, 167–174 (2016).
36. Chen, Y. & Evans, J. W. Thermal Analysis of Lithium-Ion Batteries. *J. Electrochem. Soc.* **143**, 2708 (1996).
37. Gu, W. B. & Wang, C. Y. Thermal-Electrochemical Modeling of Battery Systems. *J. Electrochem. Soc.* **147**, 2910 (2000).
38. Newman, J. & Tiedemann, W. Temperature Rise in a Battery Module with Constant Heat Generation. *J. Electrochem. Soc.* **142**, 1054 (1995).
39. Pals, C. R. & Newman, J. Thermal Modeling of the Lithium/Polymer Battery. *J. Electrochem. Soc.* **142**, 3282 (1995).
40. Rao, L. & Newman, J. Heat-Generation Rate and General Energy Balance for Insertion Battery Systems. *J. Electrochem. Soc.* **144**, 2697 (1997).
41. Spotnitz, R. & Franklin, J. Abuse behavior of high power, lithium-ion cells. **113**, 81–100 (2003).
42. Thomas, K. E. & Newman, J. Thermal Modeling of Porous Insertion Electrodes. *J. Electrochem. Soc.* **150**, A176 (2003).
43. Chacko, S. & Chung, Y. M. Thermal Modelling of Li-Ion Polymer Battery for Electric Vehicle Drive Cycles. *J. Power Sources* **213**, 296–303 (2012).
44. Kwon, K. H., Shin, C. B., Kang, T. H. & Kim, C. S. A two-dimensional modeling of a lithium-polymer battery. *J. Power Sources* **163**, 151–157 (2006).

45. Chen, S.-C., Wang, Y.-Y. & Wan, C.-C. Thermal Analysis of Spirally Wound Lithium Batteries. *J. Electrochem. Soc.* **153**, A637 (2006).
46. Damay, N., Forgez, C., Bichat, M. P. & Friedrich, G. Thermal modeling of large prismatic LiFePO<sub>4</sub>/graphite battery. Coupled thermal and heat generation models for characterization and simulation. *J. Power Sources* **283**, 37–45 (2015).
47. Forgez, C., Vinh Do, D., Friedrich, G., Morcrette, M. & Delacourt, C. Thermal modeling of a cylindrical LiFePO<sub>4</sub>/graphite lithium-ion battery. *J. Power Sources* **195**, 2961–2968 (2010).
48. Gümüştü, E., Ekici, Ö. & Köksal, M. 3-D CFD modeling and experimental testing of thermal behavior of a Li-Ion battery. *Appl. Therm. Eng.* **120**, 484–495 (2017).
49. Jeon, D. H. & Baek, S. M. Thermal modeling of cylindrical lithium ion battery during discharge cycle. *Energy Convers. Manag.* **52**, 2973–2981 (2011).
50. Kim, U. S., Yi, J., Shin, C. B., Han, T. & Park, S. Modelling the thermal behaviour of a lithium-ion battery during charge. *J. Power Sources* **196**, 5115–5121 (2011).
51. Nieto, N., Diaz, L., Gastelurrutia, J., Alava, I., Blanco, F., Ramos, J.C., Rivas, A. Thermal Modeling of Large Format Lithium-Ion Cells. *J. Electrochem. Soc.* **160**, A212–A217 (2012).
52. Panchal, S., Dincer, I., Agelin-Chaab, M., Fraser, R. & Fowler, M. Thermal modeling and validation of temperature distributions in a prismatic lithium-ion battery at different discharge rates and varying boundary conditions. *Appl. Therm. Eng.* **96**, 190–199 (2016).

53. Samba, A., Omar, N., Gualous, H., Firouz, Y., Van den Bossche, P., Mierlo, J.V., Boubekeur, T.I. Development of an advanced two-dimensional thermal model for large size lithium-ion pouch cells. *Electrochim. Acta* **117**, 246–254 (2014).
54. Shah, K., Drake, S.J., Wetz, D.A., Ostanek, J.K., Miller, S.P., Heinzl, J.M., Jain, A. An experimentally validated transient thermal model for cylindrical Li-ion cells. *J. Power Sources* **271**, 262–268 (2014).
55. Walker, W. & Ardebili, H. Thermo-electrochemical analysis of lithium ion batteries for space applications using Thermal Desktop. *J. Power Sources* **269**, 486–497 (2014).
56. Fu, R., Choe, S. Y., Agubra, V. & Fergus, J. Development of a physics-based degradation model for lithium ion polymer batteries considering side reactions. *J. Power Sources* **278**, 506–521 (2015).
57. Fuller, T. F. Simulation and Optimization of the Dual Lithium Ion Insertion Cell. *J. Electrochem. Soc.* **141**, 1 (1994).
58. Gerver, R. & Meyers, J. P. Three-Dimensional Modeling of Electrochemical Performance and Heat Generation of Spirally and Prismatic Wound Lithium-Ion Batteries. *J. Electrochem. Soc.* **160**, A1931–A1943 (2013).
59. Ghalkhani, M., Bahiraei, F., Nazri, G. A. & Saif, M. Electrochemical–Thermal Model of Pouch-type Lithium-ion Batteries. *Electrochim. Acta* **247**, 569–587 (2017).
60. Guo, M. & White, R. E. Mathematical model for a spirally-wound lithium-ion cell. *J. Power Sources* **250**, 220–235 (2014).

61. Jeon, D. H. Numerical modeling of lithium ion battery for predicting thermal behavior in a cylindrical cell. *Curr. Appl. Phys.* **14**, 196–205 (2014).
62. Jiang, F., Peng, P. & Sun, Y. Thermal analyses of LiFePO<sub>4</sub>/graphite battery discharge processes. *J. Power Sources* **243**, 181–194 (2013).
63. Kumaresan, K., Sikha, G. & White, R. E. Thermal Model for a Li-Ion Cell. *J. Electrochem. Soc.* **155**, A164 (2008).
64. Lee, C. H., Bae, S. J. & Jang, M. A study on effect of lithium ion battery design variables upon features of thermal-runaway using mathematical model and simulation. *J. Power Sources* **293**, 498–510 (2015).
65. Li, X., Xiao, M. & Choe, S. Y. Reduced order model (ROM) of a pouch type lithium polymer battery based on electrochemical thermal principles for real time applications. *Electrochim. Acta* **97**, 66–78 (2013).
66. Wang, C.-W. & Sastry, A. M. Mesoscale Modeling of a Li-Ion Polymer Cell. *J. Electrochem. Soc.* **154**, A1035 (2007).
67. Ye, Y., Shi, Y., Cai, N., Lee, J. & He, X. Electro-thermal modeling and experimental validation for lithium ion battery. *J. Power Sources* **199**, 227–238 (2012).
68. Zhang, X. Thermal analysis of a cylindrical lithium-ion battery. *Electrochim. Acta* **56**, 1246–1255 (2011).
69. Zhu, C., Li, X., Song, L. & Xiang, L. Development of a theoretically based thermal model for lithium ion battery pack. *J. Power Sources* **223**, 155–164 (2013).

70. Al-Hallaj, S., Maleki, H., Hong, J.S., Selman, J.R. Thermal Modeling and Design Considerations of Lithium-Ion Batteries. *J. Power Sources* **83**, 1–8 (1999).
71. Chen, M., Sun, Q., Li, Y., Wu, K., Liu, B., Peng, P., Wang, Q. A thermal runaway simulation on a lithium titanate battery and the battery module. *Energies* **8**, 490–500 (2015).
72. Guo, G., Long, B., Cheng, B., Zhou, S., Xu, P., Cao, B. Three-dimensional thermal finite element modeling of lithium-ion battery in thermal abuse application. *J. Power Sources* **195**, 2393–2398 (2010).
73. Larsson, F., Anderson, J., Andersson, P. & Mellander, B.-E. Thermal Modelling of Cell-to-Cell Fire Propagation and Cascading Thermal Runaway Failure Effects for Lithium-Ion Battery Cells and Modules Using Fire Walls. *J. Electrochem. Soc.* **163**, A2854–A2865 (2016).
74. Ren, D., Feng, X., Lu, L., Ouyang, M., Zheng, S., Li, J., He, X. An electrochemical-thermal coupled overcharge-to-thermal-runaway model for lithium ion battery. *J. Power Sources* **364**, 328–340 (2017).
75. Yayathi, S., Walker, W., Doughty, D. & Ardebili, H. Energy distributions exhibited during thermal runaway of commercial lithium ion batteries used for human spaceflight applications. *J. Power Sources* **329**, 197–206 (2016).
76. Zhao, W., Luo, G. & Wang, C.-Y. Modeling Nail Penetration Process in Large-Format Li-Ion Cells. *J. Electrochem. Soc.* **162**, A207–A217 (2014).
77. Tanaka, N. & Bessler, W. G. Numerical investigation of kinetic mechanism for runaway thermo-electrochemistry in lithium-ion cells. *Solid State Ionics* **262**, 70–73 (2014).

